



Scholars Research Library

Archives of Applied Science Research, 2013, 5 (5):55-61
(<http://scholarsresearchlibrary.com/archive.html>)



HMF2 quiet time variations at Ouagadougou and comparison with IRI-2012 and TIEGCM predictions during solar minimum and maximum

Emmanuel Nanéma^{1,2} and Frédéric Ouattara^{1*}

¹Laboratoire d'Enseignement et de Recherche en Sciences Expérimentales et Mathématiques (LERSEM),
Ecole Normale Supérieure de l'Université de Koudougou, BP 376 Koudougou Burkina Faso
²IRSAT/CNRST 03 BP 7047 Ouagadougou 03, Ouagadougou, Burkina Faso

ABSTRACT

The paper focuses on Ouagadougou ionosonde station quiet time hmF2 variability during solar cycle minimum and maximum and over seasons. Experimental hmF2 have been estimated by means of IRI-2012 and TIEGCM for the years 1985 and 1990. It emerges from this study that daytime peak amplitude is always superior to that of nighttime during solar minimum for both models while during solar maximum nighttime peak is always higher for TIEGCM and fairly the same for IRI-2012 for all seasons except for June where it is the reverse. hmF2 for solar maximum is higher than for solar minimum. Equinoctial asymmetry is observed during all solar phases. The pre-post sunrise peak is only observed in TIEGCM predictions. The annual anomaly is only seen during solar maximum for all models. TIEGCM better expresses data quiet time variation than IRI-2012 for this African EIA sector station.

Keywords: hmF2, IRI-2012, TIEGCM, Quiet time conditions, solar cycle minimum and maximum phases

INTRODUCTION

In African sector the IRI (International Reference ionosphere) responses have been investigated [1-3] and the 2007 version investigation [3] shows that its responses for foF2 time variations need to be improved since on one end the trough observed around midday is not so deep as seen in experimental time profile and on the other hand IRI-2007 does not predict the night peak due to the signature of the Pre-reversal enhancement of ExB drift velocity [4]. The present paper aims is to analyze a new version of IRI i.e. IRI-2012 responses through hmF2 time variations. At the same time we compare IRI-2012 predictions to those of TIEGCM (Thermosphere Ionosphere Electrodynamics General Calculation Model). TIEGCM has been intensively used for ionosphere and thermosphere study [5-11] during this decade and that usually not for African sector. Recently TIEGCM model predictions for Ouagadougou station has been analyzed [12] and it is found that the model does not reproduce the morning peak observed in experimental NmF2 time profile while the second experimental peak is more matched. The reversal time profile is better reproduced by the model.

This work investigates the seasonal and low and high solar activity hmF2 time variations carried out by IRI-2012 and TIEGCM for Ouagadougou station (lat: 12.4° N; long : 358.5°E, dip: 1.43° for 2013) under quiet geomagnetic conditions. The comparison between the both models is also made. We firstly succinctly describe the model and secondly present and discuss the result and thirdly conclude.

MATERIALS AND METHODS

2.1 Data

The data used are: (1) the propagation factor M(3000)F2, the critical frequencies of F2 and E layers of Ouagadougou (lat: 12.4° N; long : 358.5°E, dip: 1.43° for 2013) station, (2) the daily values of the geomagnetic index aa computed by Mayaud [13-14] and (3) the sunspot number Rz.

M(3000)F2 values are taken from <http://www.ips.gov.au/IPSHosted/INAG/web-73/index.html>, the daily mean aa value (Aa) and the sunspot number Rz can be found at SPIDR web site. The critical frequencies are provided by Telecom Bretagne.

2.2 IRI and TIEGCM models

IRI model is the reference model of Ionosphere. Since its creation, it has been improved up to obtaining now the version 2012. The improved model is given to the users every five years [15]. Two principal subprograms CCIR (Comité Consultatif International des Radio communications) [16-17] and URSI (Union Radio Scientifique Internationale) [18-21] are destined to reproduce main parameters of ionosphere. IRI is used to: (1) conceive experimental measures; (2) estimate ionospheric environments and its effects and at last (3) validate different theory' hypotheses. This model is independent from theoretical hypotheses; it is built by taking into account confirmed experimental results [22].

The Thermosphere-Ionosphere-Electrodynamics General Circulation Model (TIEGCM) is developed by High Altitude Observatory (HAO) at the National Center for Atmospheric Research (NCAR). It is a global three-dimensional numerical model that simulates the coupled thermosphere/ionosphere system from ~97 km to ~600 km altitude [23]. Dickinson et al. [24-25] and Roble et al. [26] developed the original version of the model i.e. Thermosphere General Circulation Model (TGCM) [23]. According to Qian et al. [23] three subsequent major developments were (1) the coupling of the ionosphere to the thermosphere in the Thermosphere-Ionosphere General Circulation Model (TIGCM) [27-28]; (2) the implementation of self-consistent electrodynamics in the Thermosphere-Ionosphere-Electrodynamics General Circulation Model (TIEGCM) [29-30] and (3) extension downward to include the mesosphere and upper stratosphere in the Thermosphere-Ionosphere-Mesosphere-Electrodynamics General Circulation Model (TIME-GCM) [31-32]. The present study concerns TIEGCM model predictions.

2.3 Methodology

For the determination of F2 layer peak height (hmF2), we follow Hoque and Jakowski [33] method that has been originally given by Radicella and Zhang [34] who used Dudeney [35-36] formula. As we have experimental data of foF2 and foE (this value is always not equal to zero in our case), Hoque and Jakowski [33] formula become:

$$hmF2 = \frac{1490 MF}{M + \Delta M} - 176 \quad \text{with} \quad \Delta M = \frac{0.253}{\frac{foF2}{foE} - 1.215} - 0.012 \quad \text{and} \quad MF = M \sqrt{\frac{0.0196 M^2 + 1}{1.2967 M^2 - 1}}$$

In these equations foF2 and foE are the critical frequencies of F2 layer and E layer, respectively. M is the propagation factor M(3000)F2. It is important to note that we do not calculate the values of foE as it has been done by Hoque and Jakowski [33] but the values are coming from our data base.

hmF2 time variation is carried out under quiet time conditions given by Aa inferior to 20 nT. The monthly hmF2 is obtained by averaging the five quietest daily values of hmF2 in a considered month. Table 1 gives the quietest days involved in the present study.

IRI-2012 hmF2 values are obtained by running the online model through the web site:

As according to the previous work [3], the subroutine URSI predictions are better than those of CCIR, therefore URSI predictions are used here.

TIEGCM hmF2 values are computed and back up via the computing service of High Altitude Observatory (HAO) at National Center for Atmospheric Research (NACAR). This has been done during our stay at HAO. After baking up the data we elaborated our own Matlab script that gives the model predicted values plotted here.

Table 1 : The days involved in the study

Months	Solar cycle phase five quietest days									
	Solar minimum Year 1985					Solar maximum Year 1990				
<i>March</i>	11	19	20	21	23	4	10	16	17	31
<i>June</i>	1	3	12	14	16	16	17	20	21	30
<i>September</i>	1	2	3	27	29	2	3	27	29	30
<i>December</i>	20	22	24	25	28	10	11	19	21	29

hmF2 predicted values are compared with those of TIEGCM during solar minimum and maximum. Solar cycle phases are determined as follows [37]: (1) minimum phase: $Rz < 20$, where Rz is the yearly average Zürich Sunspot number and (2) maximum phase: $Rz > 100$ [for small solar cycles (solar cycles with sunspot number maximum (Rz max) less than 100) the maximum phase is obtained by considering $Rz > 0.8 * Rz$ max]. For this paper we considered solar cycle 22 and particularly 1995 as solar minimum year and 1990 as that of solar maximum.

The prediction time variations are analyzed according to different seasons. Our seasons are winter (November, December, and January), spring (February, March and April), summer (May, June and July) and autumn (August, September and October). We chose March as spring month, September as autumn month, June as summer month and December as winter month. Equinoctial months are March and September and solstice months June and December.

RESULTS AND DISCUSSION

Figure 1 concerns solar minimum and figure 2 solar maximum. Panels a are devoted to equinoctial months and panels b to solstice months. Left panels a and b show hmF2 time variation for March and June, respectively. Right panels a and b exhibit the variability of hmF2 for September and December, respectively. Blue curves concern data, IRI-2012 predictions are given by red graphs while the green graphs are devoted to those of TIEGCM.

The all predicted graphs of the figure 1 exhibit dome profile with more or less high nighttime peak. The experimental curves show in March and September plateau profile and fairly dome profile in June and December. Data graphs shows in June and solstice months a pronounced pre-sunrise peak and more or less pronounced nighttime peak. June nighttime peak is the highest. It can be observed that only TIEGCM hmF2 time profiles show the pre-sunrise peak as data time profiles.

For all seasons TIEGCM better predicts experimental time profiles except between 1200 LT and 1700 LT where IRI-2012 better predicts.

In equinox (panels a), we observe the asymmetry in the hmF2 time profile morphology for all predicted and data curves. This has been also observed in CODG TEC estimated at Niamey (Geo Lat 13°28'45.3"N; Geo long: 02°10'59.5"E) [3] and has been attributed to McPherron mechanism.

Based on the existence of the linear relationship between F2 layer peak height and the scale height of the same layer [38] we can assert that the morning peak observed in hmF2 is the shape change of electron profile produces by the solar production at higher altitudes [39]. As this peak is only observed in TIEGCM predictions, it can be concluded that IRI-2012 does not reproduce the solar production effect in equatorial sector during solar cycle minimum. Comparing our results with these of the study of Lee and Reinisch [38] this effect is smallest in African sector than in American sector except during December where it is the reverse. The nighttime peak observed in all predicted and data graphs is due to the pre-reversal enhancement of ExB drift velocity [40-41]. The same thing is also seen in scale height time profile by Lee and Reinisch [38]. There is no annual anomaly because hmF2 in June (summer) is higher than in December (winter). This situation is also observed by Zhang et al.[42] in hmF2 time variation. The decreasing of hmF2 observed in TIEGCM predictions and experimental data time profiles after sunrise is related to rapid production of ionization in the lowest F region [43]. The decreasing in TIEGCM and data profiles is observed between 0500 LT and 0700 LT while Zhang et al. [42] observed this situation till 0800 LT. We do not observed here the "W" or "V" time profiles as Zhang et al. [42] because our daytime peak is higher than the two others (pre-sunrise and post-sunset peaks) except in June data graph (left panel b).

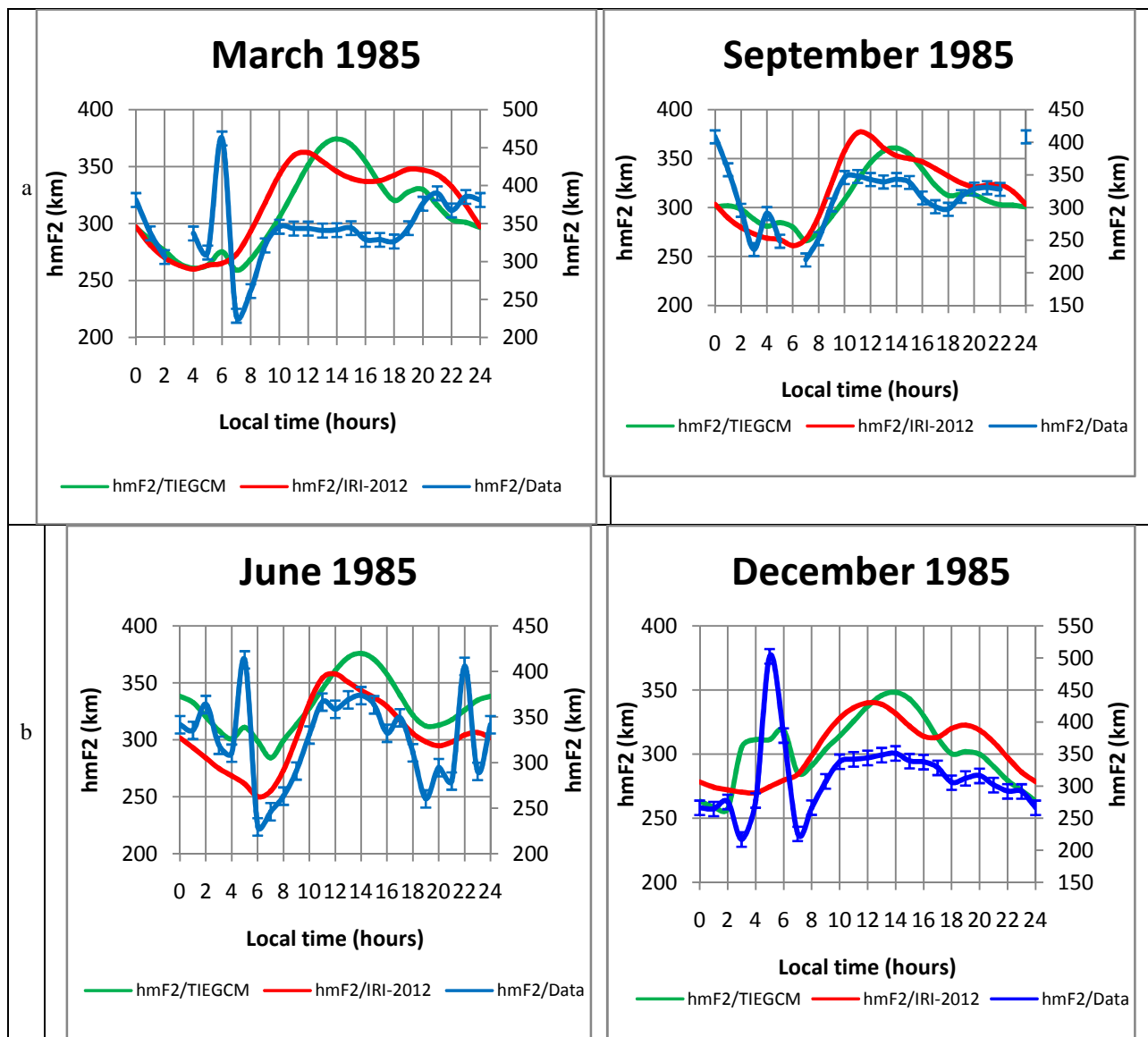


Figure 1: Quiet hmF2 time variations for solar minimum. Panels a concern equinox months and panels b for solstice months
 Left panels a and b are devoted to March and June, respectively and right panels a and b display September and December, respectively

In Figure 2, for all seasons, experimental hmF2 shows at day time fairly plateau time profile while IRI-2012 hmF2 time profiles show double peaks with trough located at 1500 LT- 1800 LT. Only in June (left panel b) this model time profile expresses the first predominance peak. TIEGCM time profiles also show double peak with trough at 1800 LT and predominance nighttime peak except in June where the both peaks fairly have the same amplitude.

Only the pre-sunrise peak is observed in TIEGCM profiles and data profiles for all seasons except in March where at 0600 LT data profile shows a trough and that of TIEGCM a peak. It can be seen that only in March the nighttime peak occurs in data time profile one hour later than in model profiles. Between 1300 LT-1800 LT IRI-2012 well expresses data variability and for the other times it is TIEGCM.

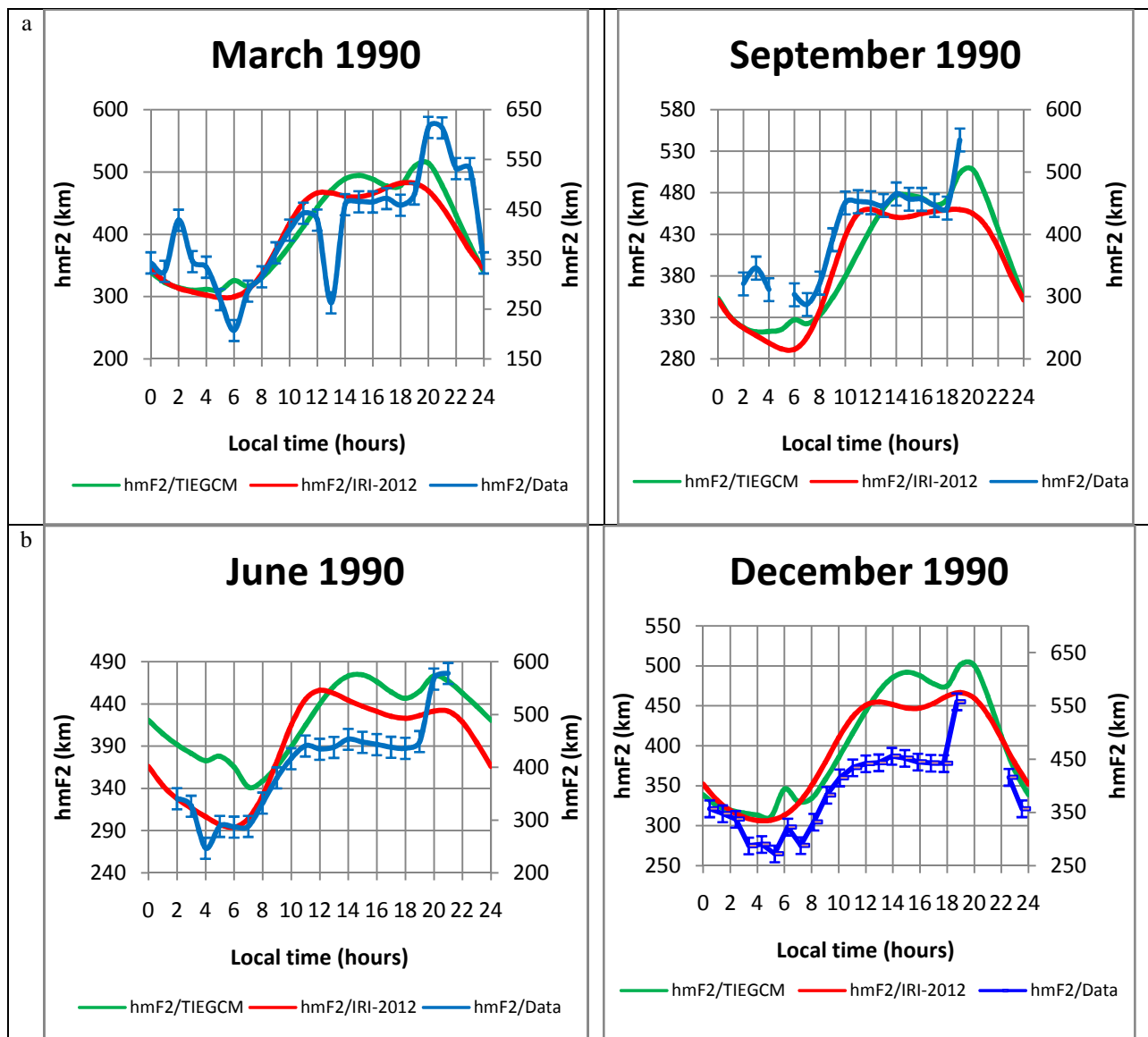


Figure 2: Quiet hmF2 time variations for solar maximum. Panels a concern equinox months and panels b for solstice months
 Left panels a and b are devoted to March and June, respectively and right panels a and b display September and December, respectively

Solar maximum curve profiles are different to those of solar minimum as the nighttime peak is higher than that of pre-sunrise in solar maximum and in solar minimum it is the reverse. This result is different to that the observation at Jicamarca where daytime peak is always higher [38].

March time profile amplitudes are superior to those of September. It emerges that there is equinoctial asymmetry during solar maximum. Theoretical graphs of solstice month express the annual anomaly as December hmF2 amplitudes are higher than those of June while this anomaly is not present in the data time profile. The annual anomaly is more pronounced in TIEGCM graphs than in those of IRI-2012. This annual anomaly is also pointed out in CODG TEC responses for this station [44] and at Koudougou station[45]. It is well known that this anomaly may be due to the presence of more ionosphere in January than in July [46]. Many explanations exist [47-49] but cannot explain the real amplitude of the annual asymmetry in all latitudes.

hmF2 is higher for the solar maximum than for the solar minimum. This situation is also observed by Zhang et al. [42]

CONCLUSION

This study highlights that solar maximum hmF2 is always superior to that of solar minimum. TIEGCM predicts well Ouagadougou station hmF2. Equinoctial asymmetry is observed for all solar cycles. Daytime peak is more expressed than that of night during solar minimum and it is the reverse during solar maximum and this specifically for TIEGM predictions. For IRI-2012 predictions daytime peak amplitudes are superior to those of nighttime during solar minimum but during solar maximum the double peak (day time and nighttime) are fairly the same amplitude except during June where the day time peak amplitude is superior to the nighttime one. In experimental graphs, nighttime peak amplitude always is superior to that of day time during solar maximum. For solar minimum, March and June daytime peak amplitudes are superior to those of nighttime while in September and December it is the reverse.

Acknowledgements

We thank Arthur D. Richmond and Astrid Maute at HAO/NCAR for their helps, advice, explanations and availability for running TIEGCM. Many thanks to HAO team for hosting us. Thank you to IRI website managers for the model availability and accessibility. Many thanks to France Telecom for providing the ionosonde data.

REFERENCES

- [1] J.O. Adeniyi, I.A. Adimula, *Adv. Space Res.*, **1995**, 15, 1441–1444
- [2] F. Ouattara, R. Fleury, *Scientific Research and Essays*, **2011**, 6, 17, 3609-3622
- [3] F. Ouattara, *Archives of Physics Research*, **2013**, 4, 3, 12-18
- [4] D.T. Farley, E. Bonell, B.G. Fejer, M.F. Larsen, *J. Geophys. Res.*, **1986**, 91, NO A12, 13,723-13,728,
- [5] G. Crowley, D. J. Knipp, K. A. Drake, J. Lei, E. Sutton, H. Luhr *Geophys. Res. Lett.*, **2010**, 37, L07110, doi: 10.1029/2009GL042143.
- [6] W. Wang, J. Lei, A. G. Burns, S. C. Solomon, M. Wiltberger, J. Xu, Y. Zhang, L. Paxton, A. Coster, *J. Geophys. Res.*, **2010**, 115, A07321, 2010, doi:10.1029/2009JA014461.
- [7] J. Lei, J. P. Thayer, A. G. Burns, G. Lu, Y. Deng, *J. Geophys. Res.*, **2010**, 115, A05303, doi:10.1029/2009JA014754.
- [8] N.M. Pedatella, J. M. Forbes, A. Maute, A. D. Richmond, T.-W. Fang, K. M. Larson, G. Millward, *J. Geophys. Res.*, **2011**, 116, A12309, doi:10.1029/2011JA016600
- [9] L. Qian, A. G. Burns, S. C. Solomon, and P. C. Chamberlin, “Solar flare impacts on ionospheric electrodyamics,” *Geophys. Res. Lett.*, **2012**, 39, L06101, doi:10.1029/2012GL051102.
- [10] A. G. Burns, S. C. Solomon, L. Qian, W. Wang, B. A. Emery, M. Wiltberger, D. R. Weimer, *J. Atmos. Solar-Terr. Phys.*, **2012**, doi:10.1016/j.jastp.2012.02.006.
- [11] S. C. Solomon, A. G. Burns, B. A. Emery, M. G. Mlynczak, L. Qian, W. Wang, D. R. Weimer, M. Wiltberger, *J. Geophys. Res.*, **2012**, doi:10.1029/2011JA017417.
- [12] E. Nanéma, A. Maute, F. Ouattara, A.D. Richmond, to be submitted, **2013**
- [13] F. Bertoni, Y. Sahai, W.L.C. Lima, P.R. Fagundes, V.G. Pillat, F. Becker-Guedes, J.R. Abalde, *Ann. Geophys.*, **2006**, 24, 2191-2200.
- [14] CCIR, Report, *Int. Telecommun. Union*, **1967**, Geneva, 340-344
- [15] CCIR, Report, *Int. Telecommun. Union*, **1991**, Geneva, 340-634
- [16] C. M. Rush, M. Pokempner, D.N. Anderson, F.G. Stewart, J.C. Perry, *Radio Sci.*, **1984**, 18, 95-107.
- [17] C. M. Rush, M. Pokempner, D.N. Anderson, J.C. Perry, F.G. Stewart, R. Reasoner, *Radio Sci.* **1984**, 19, 1083-1097.
- [18] C. M. Rush, M. Fox, D. Bilitza, K. Davies, L. McNamara, F. Stewart, M. Pokempner, *Telecomm. J.*, **1989**, 56, 179-182.
- [19] M.W. Fox, L.F. McNamara, *J. Atmos. Terr. Phys.*, **1988**, 50, 1077-1086
- [20] K.O. Obrou, PhD Thesis, Université de Cocody (Abidjan, Côte d’Ivoire, 2008).
- [21] L. Qian, A. G. Burns, B. A. Emery, B. Foster, G. Lu, A. Maute, A. D. Richmond, R. G. Roble, S. C. Solomon, W. Wang, submitted to *AGU Geophysical Monograph Series*, **2012**
- [22] R. E. Dickinson, E. C. Ridley, R. G. Roble, *J. Geophys. Res.*, **1981**, 86, 1499-1512.
- [23] R. E. Dickinson, E. C. Ridley, R. G. Roble, *J. Atmos. Sci.*, **1984**, 41, 205-219
- [24] R. G., Roble, E. C. Ridley, R. E. Dickinson, *J. Geophys. Res.*, **1982**, 87, 1599-1614.
- [25] R. G. Roble and E. C. Ridley, *Annales. Geophysicae*, **1987**, 5A, 6, 369-382.
- [26] R. G. Roble, E. C. Ridley, A. D. Richmond, R. E. Dickinson, *Geophys. Res. Lett.*, **1988**, 15, 1325
- [27] A. D. Richmond, E. C. Ridley, R. G. Roble, *Geophys. Res. Lett.*, **1992**, 19, 601,
- [28] A. D. Richmond, *J. Geomagn. Geoelectr.*, **1995**, 47, 191-212.

- [29] R. G. Roble, E. C. Ridley, *Geophys. Res. Lett.*, **1994**, 21, 417
- [30] R. G. Roble, *Geophys. Mono.*, **1995**, 87, 1-21.
- [31] P.N. Mayaud, *Ann. Geophys.*, **1971**, 27, 71-73
- [32] P. N. Mayaud, 1973. *IGA Bull.*, 33, Zurich, 251
- [33] M.M. Hoque, N. Jakowski, *Annales Geophysicae*, **2012**, 30, 797-809
- [34] S.-R. Zhang, W. L. Oliver, J. M. Holt, S. Fukao, *J. Geophys. Res.*, 2003, 108, 1131, doi:10.1029/2002JA009521
- [35] J. R. Dudeney, *J. Atmos. Terr. Phys.*, **1978**, 40, 195–203
- [36] J. R. Dudeney, *J. Atmos. Terr. Phys.*, **1983**, 45, 629–640, doi:10.1016/S0021-9169(83)80080-4
- [37] F. Ouattara, *British Journal of Applied Science and Technology*, **2012**, 2, 3, 240-253
- [38] C.C Lee, B.W. Reinisch, *Ann. Geophys.*, **2007**, 25, 2541-2550
- [39] C. C. Lee, B.W. Reinisch, S.-Y Su, W.S. Chen, *J. Atmos. Terr. Phys.*, **2007**, 74, 217-223.
- [40] B.G. Fejer, *J. Atmos. Terr. Phys.*, **1981**, 43, 377
- [41] S.-R. Zhang, S. Fukao, W.L. Oliver, Y. Otsuka, *J. Atmos. Terr. Phy*, **1999**, 61, 1367-1383
- [42] H. Rishbeth, O.K. Gariott, Introduction to Ionospheric Physics, Academic Press, New York and London, **1969**
- [43] C. Zoundi, F. Ouattara, E. Nanéma, R. Fleury, F. Zougmore, *European Scientific Journal*, to be appeared, **2013**
- [44] F. Ouattara, C. Zoundi, R. Fleury, *Indian Journal of Radio and Space Physics*, **2013**, 41, 617-623
- [45] H. Rishbeth, I.C.F. Muller-Wodarg, *Ann. Geophys.*, **2006**, 24, 3293–3311
- [46] T. Yonezawa, Y. Arima, *J. Radio Res. Labs.*, **1959**, 6, 293–309
- [47] M.J. Buonsanto, *S. Pacific J. Nat. Sci.*, **1986**, 8, 58–65
- [48] H. Rishbeth, I.C.F. Muller-Wodarg, L. Zou, T.J. Fuller-Rowell, G.H. Millward, R.J., Moffett, D.W Idenden, A.D. Aylward, *Ann. Geophys.*, **2000**, 18, 945–956